

Citation for published version:

Anastasios Papazafeiropoulos, Shree Krishna Sharma, Tharmalingam Ratnarajah, and Symeon Chatzinotas, 'Impact of Residual Additive Transceiver Hardware Impairments on Rayleigh-Product MIMO Channels With Linear Receivers: Exact and Asymptotic Analyses', *IEEE Transactions on Communications*, Vol. 66 (1): 105-118, January 2018.

DOI:

<https://doi.org/10.1109/TCOMM.2017.2753773>

Document Version:

This is the Accepted Manuscript version.

The version in the University of Hertfordshire Research Archive may differ from the final published version.

Copyright and Reuse:

© 2017 IEEE

Personal use of this material is permitted. Permission from IEEE must be obtained for all other uses, in any current or future media, including reprinting/republishing this material for advertising or promotional purposes, creating new collective works, for resale or redistribution to servers or lists, or reuse of any copyrighted component of this work in other works.

Enquiries

If you believe this document infringes copyright, please contact the Research & Scholarly Communications Team at rsc@herts.ac.uk

Impact of Residual Additive Transceiver Hardware Impairments on Rayleigh-Product MIMO Channels with Linear Receivers: Exact and Asymptotic Analyses

Anastasios Papazafeiropoulos, *Member, IEEE*, Shree Krishna Sharma, *Member, IEEE*, Tharmalingam Ratnarajah, *Senior Member, IEEE*, and Symeon Chatzinotas, *Member, IEEE*,

Abstract—Despite the importance of Rayleigh-product multiple-input multiple-output (MIMO) channels and their experimental validations, there is no work investigating their performance in the presence of residual additive transceiver hardware impairments, which arise in practical scenarios. Hence, this paper focuses on the impact of these residual imperfections on the ergodic channel capacity for optimal receivers, and on the ergodic sum-rates for linear minimum mean-squared-error (MMSE) receivers. Moreover, the low and high-signal-to-noise ratio (SNR) cornerstones are characterized for both types of receivers. Simple closed-form expressions are obtained that allow the extraction of interesting conclusions. For example, the minimum transmit energy per information bit for optimal and MMSE receivers are not subject to any additive impairments. In addition to the exact analysis, we also study the Rayleigh-Product channels in the large system regime, and we elaborate on the behavior of the ergodic channel capacity with optimal receivers by varying the severity of the transceiver additive impairments.

Index Terms—Ergodic capacity, Rayleigh-product channels, hardware impairments, massive MIMO, MMSE receivers.

I. INTRODUCTION

Multiple-input multiple-output (MIMO) systems have received an enormous attention in terms of understanding the fundamental capacity limits of various models [2]–[4]. However, the potential benefits of MIMO have been mostly considered in rich scattering conditions, described by a full rank channel matrix. In practice, there are environments, where the “richness” is not fulfilled due to insufficient scattering [5]

Anastasios Papazafeiropoulos and Tharm Ratnarajah are with the Institute for Digital Communications (IDCOM), The University of Edinburgh, Edinburgh EH9 3JL, U.K. Shree Krishna Sharma is with the Department of Electrical and Computer Engineering, Western University, Canada. Symeon Chatzinotas is with the SnT - securityandtrust.lu, University of Luxembourg, Luxembourg, (Email: a.papazafeiropoulos, t.ratnarajah@ed.ac.uk), sshar323@uwo.ca, and symeon.chatzinotas@uni.lu.

Parts of this work were presented in IEEE International workshop on Signal Processing Advances in Wireless Communications, Edinburgh, U.K., Jul. 2016 [1].

Copyright (c) 2017 IEEE. Personal use of this material is permitted. However, permission to use this material for any other purposes must be obtained from the IEEE by sending a request to pubs-permissions@ieee.org.

This work was supported by the U.K. Engineering and Physical Sciences Research Council (EPSRC) under grant EP/L025299/1. The work of S. K. Sharma and S. Chatzinotas was partially supported by the projects H2020 SANSA and FNR SATSENT, SEMIGOD, INWIPNET, PROSAT.

or the “keyhole” effect [6]. In such cases, a rank deficiency, concerning the channel matrix, appears. The physical explanation behind this rank deficiency is the description of the double scattering effect¹ [6]–[13]. This phenomenon was experimentally validated in [8], [9], [11], while its mathematical characterization is given by the product of two statistically independent complex Gaussian matrices. Interestingly, when the antenna elements and the scattering objects are sufficiently separated, the effective spatial correlations can be ignored, resulting in the Rayleigh-product model².

Plenty of works have studied the double scattering models in different settings, and in particular, the double Rayleigh model, which is the special case of double scattering model with identity transmitter, scatter and receiver correlation matrices. For example, the derivation of an ergodic capacity upper bound for this channel was carried out in [13]. In particular, its performance with the low complexity linear minimum mean-squared-error (MMSE) receivers was investigated recently in [14]. However, the misleading standard assumption in the context of double Rayleigh channels, considered in the existing literature, includes ideal transceiver hardware, which is far from reality.

Inevitably, practical transceivers present hardware imperfections such as high power amplifier non-linearities and in-phase/quadrature (I/Q) imbalance [15]–[26]. The hardware impairments can be mainly classified into two categories. In the first category, the effect of hardware impairments is modeled as a multiplicative factor to the channel vector causing channel attenuation and phase shifts. Note that this factor cannot be incorporated by the channel vector by an appropriate scaling of its covariance matrix or due to the property of circular symmetry of the channel distribution,

¹The double scattering effect includes both rank-deficiency and spatial correlation.

²It should be noted that the Rayleigh product channel can lead to a keyhole in the extreme case of only one scatterer. Although the keyhole channel has been studied intensively in the literature, it is still unclear how often this appears in real situations [9]. However, the Rayleigh product is a generalization of the keyhole channel and can capture a much wider range of scattering environments. In this direction, the next step would be to consider parametric channel modes which depend on the angles or transmission and arrival given a set of scattering clusters. This would require a different analytical approach since the i.i.d. properties of the channel coefficients no longer hold and it is reserved for future work.

when it changes faster than the channel. An example is the phase noise, which accumulates within the channel coherence period [18], [27]. On the other hand, the aggregate effect from many impairments can be described by an additive system model [15], [16], [22]–[26], [28], [29], where the impairments are modeled as independent additive distortion noises at the base station (BS) as well as at the user. It is a well-established model due to its analytical tractability and the experimental verifications [16]. These kind of impairments emerge as residual hardware impairments after the application of inadequate compensation algorithms. Several reasons lead to this inadequacy such as the imperfect parameter estimation caused by the randomness and the time variation of the hardware characteristics, the inaccuracy coming from limited precision models, unsophisticated compensation algorithms, etc [15], [16]. In particular, non-ideal hardware sets a finite capacity limit at high signal-to-noise ratio (SNR), where the authors considered only transmitter impairments [15], [16], [21]. The impact of additive hardware impairments has been studied for various channel models, e.g., point-to-point MIMO channels, amplify-and-forward (AF) relay systems, and heterogeneous networks [21]–[23], [28]. This paper grapples with the thorough investigation of residual additive hardware impairments in Rayleigh-product MIMO channels, while multiplicative impairments are left for future work.

Turning the focus into the emerging technology of massive MIMO, where a BS is deployed with a large number of antennas and achieves a number of interesting properties such as high gain and the ease of implementation, most works assume ideal transceiver hardware [30]–[33]. Given that massive MIMO systems are supposed to be implemented with low-cost hardware, and hence are more prone to impairments, this is a strong assumption. As a result, there is a meaningful turn of the attention towards the direction of previous study regarding the hardware impairments [27], [28]. For example, [27] showed that massive MIMO systems are more tolerant to hardware impairments. Moreover, the authors in [28], considering the additive transceiver impairments, extended the analysis of [21] to massive MIMO for arbitrary SNR values. It is worthwhile to mention that the double scattering channel has been already investigated for massive MIMO systems, which is one of the prominent technologies for 5G of [34], [35]. Moreover, it should be noted that the keyhole channel is a first step towards the double scattering channels which is a suitable model for characterizing the scattering limitations of higher frequencies envisaged in the fifth generation (5G) networks. Although these models have limitations in terms of accurately matching the measurement campaigns, we believe that they will remain useful tools for theoretical analysis of wireless system performance³.

In this paper, assuming that the channel state information (CSI) is not known at the transmitter side but it is perfectly known at the receiver, we focus on the investigation of the ergodic capacity with residual transceiver impairments in the context of double Rayleigh channels with optimal and linear

receivers (MMSE) in both regimes of finite and asymptotically large MIMO⁴. It is worthwhile to mention that the study of double Rayleigh channels is quite important in massive MIMO systems and millimeter wave (mmWave) communications suggested for the forthcoming 5G networks. For example, in urban environments, double Rayleigh channels are more probable, and it is crucial to investigate their realistic behavior when residual hardware impairments are considered. Due to high operating frequencies and wider bandwidths, it is important to analyze the effect of transceiver hardware impairments for the realistic performance evaluation of mmWave systems [36], [37]. In this regard, recent experimental results in the literature [37] have demonstrated that the achievable data rate in wideband mmWave systems is severely limited by the local oscillator phase noise resulted due to the multiplicative noise added while performing frequency multiplication of low-frequency local oscillator to a high frequency.

Furthermore, it is of great interest to show how the deficiency of the channel matrix, i.e., the number of scatterers affects the capacity by means of a thorough analysis in the presence of the residual impairments in both the conventional and large numbers of antennas regimes. In fact, although [14] provides a similar analysis, we clearly differentiate from this, since we incorporate the inevitable residual additive transceiver impairments. In addition, the current paper delves into the large system limit, thus leading to further insights. To the best of our knowledge, there appears to be no analytical results investigating the impact of transceiver impairments for double Rayleigh channels⁵. In this direction, this paper provides the following specific contributions:

- We study the ergodic channel capacity with optimal receivers and the achievable sum-rate with linear MMSE receivers for double Rayleigh channels in the presence of residual transceiver hardware additive impairments. Specifically, we derive novel exact analytical expressions.
- Towards obtaining more engineering insights, we further investigate the low and high-SNR regimes by deriving simple closed-form expressions for each type of receiver. These results shed more light on the performance of rank deficient channels in the realistic case, where the inevitable imperfect hardware is present.
- Based on the proposed system model, we provide the ergodic channel capacity with optimal receivers for double Rayleigh channels under the presence of residual hardware impairments in the large system limit by using a free probability (FP) analysis.

The remainder of the paper is organized as follows: Section II presents the system and signal models with both ideal and imperfect hardware. In Section III, we provide a detailed study of ergodic capacity for Rayleigh-product channels with optimal receivers including the characterization of the low and high-SNR regimes. To this direction, we perform a similar

⁴Among the linear receivers, we have chosen the MMSE receivers because they provide the higher performance with reasonable complexity, especially, in the large system regime, where the statistical expressions become deterministic.

⁵The behaviour of double Rayleigh channels in the large system limit without any transceiver hardware impairments has been studied only in [34].

³It is worthwhile to mention with a fair degree of caution that this model has not been validated by measurements and at this stage, it should be treated as a proposed model rather than the correct model.

analysis for the sum-rate of linear MMSE receivers in Section IV. With concern to the large system limit, where the numbers of antennas and scatterers tend to infinity, but with a given ratio, Section V elaborates on the investigation of Rayleigh-product MIMO channels in the presence of hardware impairments in the large antenna regime. Finally, concluding remarks are given in Section VI.

Notation: Vectors and matrices are denoted by boldface lower and upper case symbols. The \otimes symbol denotes the Kronecker product. The transpose, Hermitian transpose, and trace operators are represented by $(\cdot)^T$, $(\cdot)^H$, and $\text{tr}(\cdot)$, respectively. Additionally, $\Gamma(z) = \int_0^\infty t^{z-1} e^{-t} dt$ and $G_{p,q}^{m,n}(x | \begin{smallmatrix} \alpha_1, \dots, \alpha_p \\ \beta_1, \dots, \beta_q \end{smallmatrix})$ are the Gamma function [38, Eq. 8.310] and the Meijer G-function [38, Eq. 9.301], respectively. The form of \mathbf{A}/\mathbf{B} , where \mathbf{A} and \mathbf{B} are matrices, denotes $\mathbf{A}\mathbf{B}^{-1}$ with \mathbf{B}^{-1} standing for the inverse of the matrix \mathbf{B} . The first and the second derivatives are denoted by $\frac{\partial}{\partial p}$ or $(\cdot)'$ and $\frac{\partial^2}{\partial p^2}$ or $(\cdot)''$, respectively. The expectation operator and the determinant of a matrix are denoted by $\mathbb{E}[\cdot]$ and $\det(\cdot)$, respectively. The notations \mathcal{C}^M and $\mathcal{C}^{M \times N}$ refer to complex M -dimensional vectors and $M \times N$ matrices, respectively. The $\text{diag}\{\cdot\}$ operator generates a diagonal matrix from a given vector, and \mathbf{I}_N denotes the identity matrix of size N . Moreover, $\mathbf{b} \sim \mathcal{CN}(\mathbf{0}, \mathbf{\Sigma})$ denotes a circularly symmetric complex Gaussian vector with zero-mean and covariance matrix $\mathbf{\Sigma}$ signifies the positive part of its argument, while $\mathbf{X} \sim \mathcal{CN}(\mathbf{M}, \mathbf{\Sigma} \otimes \mathbf{\Psi})$ denotes that \mathbf{X} is a Gaussian distributed matrix with mean matrix $\mathbf{M} \in \mathbb{C}^{p \times q}$ and covariance matrix $\mathbf{\Sigma} \otimes \mathbf{\Psi}$ where $\mathbf{\Sigma} \in \mathbb{C}^{p \times p}$ and $\mathbf{\Psi} \in \mathbb{C}^{q \times q}$ are Hermitian matrices with $p \leq q$.

II. SYSTEM MODEL

We take into consideration the canonical flat-fading point-to-point MIMO channel with M transmit antennas and N receive antennas, as depicted in Fig. 1(a). Mathematically speaking, the received signal in vector form is written as

$$\mathbf{y} = \mathbf{H}\mathbf{x} + \mathbf{z}, \quad (1)$$

where $\mathbf{x} \in \mathcal{C}^{M \times 1}$ is the zero-mean transmit Gaussian vector with covariance matrix $\mathbb{E}[\mathbf{x}\mathbf{x}^H] = \mathbf{Q} = \frac{\rho}{M}\mathbf{I}_M$, and $\mathbf{z} \sim \mathcal{CN}(\mathbf{0}, \mathbf{I}_N)$ denotes the additive white Gaussian noise (AWGN) noise vector at the receiver. Note that ρ represents the SNR, since we have assumed that the channel gain and receiver noise power are normalized. Especially, $\mathbf{H} \in \mathbb{C}^{N \times M} \sim \mathcal{CN}(\mathbf{0}, \mathbf{I}_N \otimes \mathbf{I}_M)$ represents the Rayleigh-product MIMO channel, exhibiting flat-fading in the presence of a number of scatterers. More concretely, \mathbf{H} is described as

$$\mathbf{H} = \frac{1}{\sqrt{K}}\mathbf{H}_1\mathbf{H}_2, \quad (2)$$

where $\mathbf{H}_1 \in \mathbb{C}^{N \times K} \sim \mathcal{CN}(\mathbf{0}, \mathbf{I}_N \otimes \mathbf{I}_K)$ and $\mathbf{H}_2 \in \mathbb{C}^{K \times M} \sim \mathcal{CN}(\mathbf{0}, \mathbf{I}_K \otimes \mathbf{I}_M)$ are random matrices with K quantifying the number of scatterers in the propagation environment [6].

Unfortunately, the common assumption of ideal hardware, possibly leading to misleading results, is not realistic because both the transmitter and the receiver suffer from certain inevitable additive impairments such as I/Q imbalance and high power amplifier (HPA) nonlinearities [15]. In fact, mitigation schemes are applied at both the transmitter and the

receiver. However, the emergence of various distortion noises is unavoidable due to residual impairments [15], [16], [23], [27]. Consequently, hardware transmit impairments induce a mismatch between the intended signal and what is actually transmitted during the transmit processing, and similarly, a distortion of the received signal at the receiver side is produced due to imperfect receiver hardware. As mentioned in Section-I, these residual impairments can be modeled in terms of distortions, which can be: a) multiplicative, when the received signals are shifted in phase; b) additive, where the distortion noise is added with a power proportional to the transmit signal power and the total received signal power; and c) amplified thermal noise. A generic model, including all these hardware impairments, is written as

$$\mathbf{y}_n = \mathbf{\Theta}_n\mathbf{H}(\mathbf{\Psi}_n\mathbf{x}_n + \boldsymbol{\eta}_{t,n}) + \boldsymbol{\eta}_{r,n} + \boldsymbol{\xi}_n, \quad (3)$$

where the additive terms $\boldsymbol{\eta}_{t,n}$ and $\boldsymbol{\eta}_{r,n}$ denote the distortion noises at time n coming from the residual impairments in the M antennas transmitter and N antennas receiver, respectively, as shown in Fig. 1(b). Moreover, $\mathbf{\Theta}_n = \text{diag}\{e^{j\theta_n^{(1)}}, \dots, e^{j\theta_n^{(N)}}\} \in \mathbb{C}^{N \times N}$ is the phase noise sample matrix because of the imperfections in the local oscillators (LOs) of the receiver, while $\mathbf{\Psi}_n = \text{diag}\{e^{j\psi_n^{(1)}}, \dots, e^{j\psi_n^{(M)}}\} \in \mathbb{C}^{M \times M}$ is the the phase noise sample matrix because of the imperfections in the LOs. The phase noise expresses the distortion in the phase due to the random phase drift in the signal coming from the LOs of both the transmitter and the receiver during the up-conversion of the baseband signal to passband and vice versa. The phase noise during the n th time slot can be described by a discrete-time independent Wiener process, i.e., the phase noises at the LOs of the m th antenna of the transmitter and k th antenna of the receiver are modeled as [27]

$$\psi_{m,n} = \psi_{m,n-1} + \delta_n^{\psi_m} \quad (4)$$

$$\theta_{k,n} = \theta_{k,n-1} + \delta_n^{\theta_k}, \quad (5)$$

where $\delta_n^{\psi_m} \sim \mathcal{N}(0, \sigma_{\psi_m}^2)$ and $\delta_n^{\theta_k} \sim \mathcal{N}(0, \sigma_{\theta_k}^2)$. Note that $\sigma_i^2 = 4\pi^2 f_c c_i T_s$, $i = \psi_m, \theta_k$ describes the phase noise increment variance with T_s , c_i , and f_c being the symbol interval, a constant dependent on the oscillator, and the carrier frequency, respectively. Furthermore, some components such as the low noise amplifier and the mixers at the receiver engender an amplification of the thermal noise, which appears as an increase of its variance [27]. In fact, the total effect $\boldsymbol{\xi}_n$ can be modeled as Gaussian distributed with zero-mean and variance $\xi_n \mathbf{I}_N$, where $\sigma^2 = 1 \leq \xi_n$ is the corresponding parameter of the actual thermal noise. Note that all the impairments are time-dependent because they take new realizations for each new data signal. Remarkably, the recent work in [39] proposed the rate-splitting approach as a robust method against the residual multiplicative transceiver hardware impairments. Although these impairments are residual [39], this work showed the robustness of rate-splitting over the multiplicative impairments, while the additive impairments can be mitigated with this approach. Note that the topic of further dealing with other methods and strategies to mitigate the residual impairments is left for future work.

Focusing on the manifestation of only the residual additive transceiver impairments, the generic model, after absorbing the subscript n , becomes⁶

$$\mathbf{y} = \mathbf{H}(\mathbf{x} + \boldsymbol{\eta}_t) + \boldsymbol{\eta}_r + \mathbf{z} \quad (6)$$

$$= \mathbf{h}_m x_m + \sum_{i=1, i \neq m}^M \mathbf{h}_i x_i + \mathbf{H}\boldsymbol{\eta}_t + \boldsymbol{\eta}_r + \mathbf{z}, \quad (7)$$

where, x_m is the transmit signal from the m th transmit antenna. A general approach, validated by measurement results, considers the assumption that the transmitter and the receiver distortion noises are Gaussian distributed with their average power being proportional to the average signal power [15], [16], [28], and references therein⁷. In other words, the distortion noises are modelled as⁸

$$\boldsymbol{\eta}_t \sim \mathcal{CN}(\mathbf{0}, \delta_t^2 \text{diag}(q_1, \dots, q_M)), \quad (8)$$

$$\boldsymbol{\eta}_r \sim \mathcal{CN}(\mathbf{0}, \delta_r^2 \text{tr}(\mathbf{Q}) \mathbf{I}_N), \quad (9)$$

where δ_t^2 and δ_r^2 are proportionality parameters describing the severity of the residual impairments in the transmitter and the receiver. Moreover, q_1, \dots, q_M are the diagonal elements of the signal covariance matrix \mathbf{Q} . Hence, taking into account for the form of the covariance matrix \mathbf{Q} , the additive transceiver impairments are expressed as

$$\boldsymbol{\eta}_t \sim \mathcal{CN}(\mathbf{0}, \delta_t^2 \frac{\rho}{M} \mathbf{I}_M), \quad (10)$$

$$\boldsymbol{\eta}_r \sim \mathcal{CN}(\mathbf{0}, \delta_r^2 \rho \mathbf{I}_N). \quad (11)$$

In the following sections, we provide the theoretical analysis and we verify the analytical results with the help of numerical results. Subsequently, we illustrate the impact of impairments on the ergodic capacity of Rayleigh-product channels with optimal receivers and the ergodic sum rate of the Rayleigh-product channels with MMSE receivers.

III. ERGODIC CHANNEL CAPACITY ANALYSIS

In this section, we investigate the impact of residual hardware impairments on the ergodic channel capacity of Rayleigh-product MIMO channels with optimal receivers, when the number of antennas is arbitrary, but finite. Also, we assume

⁶Note that (7) reduces to the ideal model (1) for $\delta_t = \delta_r = 0$, which indicates ideal hardware on both sides of the transceiver.

⁷The circularly-symmetric complex Gaussianity, verified experimentally (see e.g., [40, Fig. 4.13]), can be also justified by means of the central limit theorem (CLT), since we assume the aggregate contribution of many independent impairments.

⁸Two basic approaches in the literature are followed for describing the receive distortion noises. Their difference lies on both the mathematical expression and physical meaning, where two types of randomness appear when the received power is measured. The first approach includes the channel variations, while the second one concerns the energy-variations in the waveform/modulation (the Gaussian codebook in our case). Hence, in several works (e.g., see [27]), the authors take the average over the waveform/modulation, i.e., the transmit signal, but not over the channel coefficients. For the sake of simplified mathematical exposition and analysis, in this work, we follow the second approach, where we take the average over both the channel variations and the waveform [23], [28]. Following this direction, our analysis is more tractable, while revealing at the same time all the interesting properties. It is worthwhile to mention that the model that is closest to reality does not apply any average.

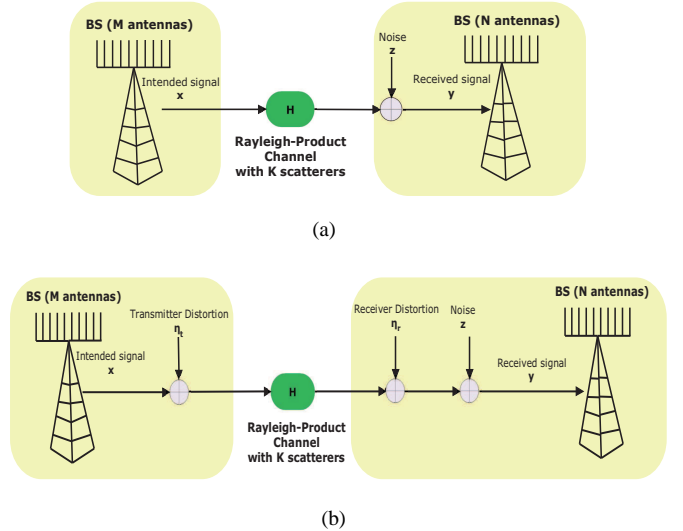


Fig. 1. (a) Conventional Rayleigh-product MIMO system with K scatterers and ideal transceiver hardware. (b) Rayleigh-product MIMO system with K scatterers and residual additive transceiver hardware impairments.

that no CSI is known at the transmitter side but it is perfectly known at the receiver. In particular, the following proposition allows us to express the ergodic capacity, when optimal receivers are employed. Actually, it provides the starting point for the subsequent derivations.

Proposition 1: The ergodic channel capacity of a practical Rayleigh-product MIMO channel with optimal linear receivers, but with residual additive transceiver impairments under the constraint $\text{tr} \mathbf{Q} \leq \rho$ is given by

$$C^{\text{opt}}(\rho, M, N, K, \delta_t, \delta_r) = \mathbb{E} \left[\log_2 \det \left(\mathbf{I}_N + \frac{\rho}{M} \mathbf{H} \mathbf{H}^H \boldsymbol{\Phi}^{-1} \right) \right], \quad (12)$$

where $\boldsymbol{\Phi} = \frac{\rho}{KM} \delta_t^2 \mathbf{H}_1 \mathbf{H}_2 \mathbf{H}_2^H \mathbf{H}_1^H + (\rho \delta_r^2 + 1) \mathbf{I}_N$.

Proof: It can be seen that (7) is an instance of the standard MIMO channel given by (2) for any channel realizations $\mathbf{H}_1, \mathbf{H}_2$ and transmit signal covariance matrix \mathbf{Q} , being a scaled identity matrix, but with a different noise covariance given by

$$\boldsymbol{\Phi} = \frac{\delta_t^2}{K} \mathbf{H}_1 \mathbf{H}_2 \text{diag}(q_1, \dots, q_M) \mathbf{H}_2^H \mathbf{H}_1^H + (\delta_r^2 \text{tr} \mathbf{Q} + 1) \mathbf{I}_N. \quad (13)$$

In such case, the ergodic capacity is written as

$$C^{\text{opt}}(\rho, M, N, K) = \max_{\mathbf{Q}: \text{tr} \mathbf{Q} \leq \rho} \mathbb{E} \left[\log_2 \det (\mathbf{I}_N + \mathbf{H} \mathbf{Q} \mathbf{H}^H \boldsymbol{\Phi}^{-1}) \right].$$

Taking into account for the sufficiency and optimality of the input signal \mathbf{x} , since it is Gaussian distributed with covariance matrix $\mathbf{Q} = \frac{\rho}{M} \mathbf{I}_M$ [2], the proof is concluded. Note that there is no need of optimization of \mathbf{Q} , since we have no CSIT. For this reason, we use unit covariance. ■

In what follows, we refer to $m = \max(M, N)$, $n = \min(M, N)$, $p = \max(m, K)$, $q = \min(m, K)$, $s = \min(K, n)$, $t = \max(K, n)$, and $\tilde{\delta}_t^2 = 1 + \delta_t^2$, as well as for notational convenience we denote $f_1(\rho) = \frac{\rho}{KM} \frac{(1 + \delta_t^2)}{\rho \delta_r^2 + 1}$ and $f_2(\rho) = \frac{\frac{\rho}{KM} \delta_t^2}{\rho \delta_r^2 + 1}$.

A. Exact Expression

Herein, we focus on the study of realistic Rayleigh-product channels with optimal receivers. In particular, the following theorem, presenting the ergodic capacity of Rayleigh-product channels with optimal receivers in the presence of hardware impairments, being one of the main contributions of this paper, is of high interest.

Theorem 1: The ergodic capacity of practical Rayleigh-product channels with optimal receivers, accounting for residual additive hardware transceiver impairments, is given by

$$\mathcal{C}^{\text{opt}}(\rho, M, N, K, \delta_t, \delta_r) = \mathcal{A}(\mathcal{C}_1(\rho, M, N, K, \delta_t, \delta_r) - \mathcal{C}_2(\rho, M, N, K, \delta_t, \delta_r)), \quad (14)$$

where

$$\mathcal{A} = \frac{\mathcal{K}}{\ln 2} \sum_{i=1}^s \sum_{j=1}^s \frac{G_{i,j}}{\Gamma(p-s+j)} \quad (15)$$

with

$$\mathcal{K} = \left(\prod_{i=1}^s \Gamma(s-i+1) \Gamma(t-i+1) \right)^{-1}, \quad (16)$$

and $G_{i,j}$ is the (i, j) th cofactor of an $s \times s$ matrix \mathbf{G} whose (u, v) th entry is

$$[G]_{u,v} = \Gamma(t-s+u+v-1).$$

Especially, regarding \mathcal{C}_i for $i = 1, 2$, we have

$$\mathcal{C}_i(\rho, M, N, K, \delta_t, \delta_r) = G_{4,2}^{1,4}(f_i | a_{1,1}, a_{2,1,1}), \quad (17)$$

where $a_1 = s + 2 - i - j - t$, and $a_2 = s + 1 - p - j$.

Proof: See Appendix B. ■

Remark 1: In the case of ideal transceiver hardware, where $\delta_t = \delta_r = 0$, Theorem 1 coincides with [14, Lemma 3].

The complicated expression of the capacity of optimal receivers, provided by Theorem 1 does not allow a simple analysis that would reveal the impact of various system parameters. Hence, we focus onto the asymptotic high and low SNR regimes. In fact, we derive simple expressions enabling valuable physical insights into the system performance.

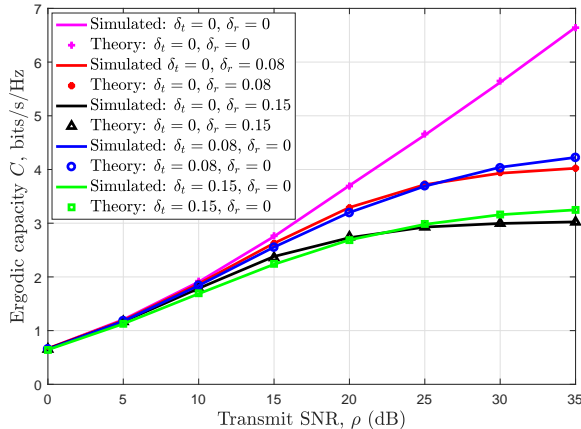


Fig. 2. Per-antenna ergodic capacity of Rayleigh product channels with optimal receivers for different levels of impairment severity at the transmitter and receiver ($K = 3$, $M = 4$, $N = 5$).

Fig. 2 presents the per-antenna ergodic capacity of Rayleigh-product channels with optimal receivers considering $K = 3$, $M = 4$, $N = 5$. Both theoretical and simulated results are presented for the cases with and without residual transceiver hardware impairments⁹. The theoretical curve for the case without impairments was obtained by following the analysis considered in [14]. Whereas, the theoretical curves for the practical case with hardware impairments were obtained by evaluating (14). Furthermore, the simulated curves were obtained by averaging the corresponding capacities over 10^3 random instances of \mathbf{H}_1 and \mathbf{H}_2 . It can be noted from Fig. 2 that the proposed capacity expression matches well with the Monte Carlo (MC) simulation for the arbitrary finite values of K , M and N . Most importantly, we note that in the absence of residual hardware impairments, i.e., $\delta_t = 0$, $\delta_r = 0$, the per-antenna ergodic capacity monotonically increases with the increase in the value of ρ . However, in the presence of residual hardware impairments, the ergodic capacity first increases with the increase in the value of ρ and then gets saturated after a certain value of ρ . Besides, the capacity gap in the presence of impairments as compared to the case without impairments increases with the increase in the value of ρ . Moreover, another important observation from Fig. 2 is that the per-antenna ergodic capacity decreases with the increase in the severity of the residual hardware impairments. In particular, the lower the quality of transceiver hardware (higher severity), the earlier the saturation point appears.

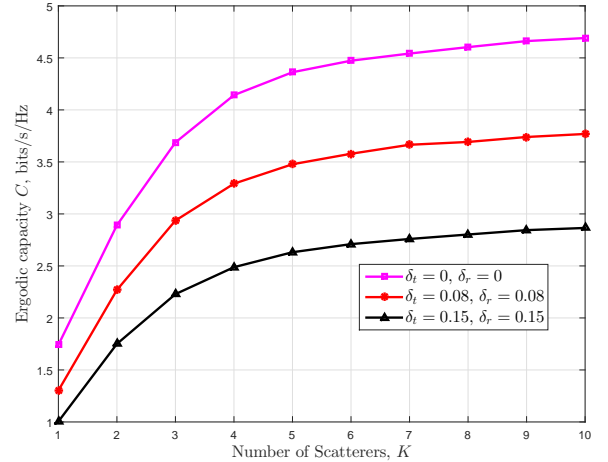


Fig. 3. Per-antenna ergodic capacity versus number of scatterers for Rayleigh product channels with optimal linear receivers ($\rho = 20$ dB, $M = 4$, $N = 5$).

In addition, Fig. 2 demonstrates the effect of different levels of impairments at the transmitter and receiver sides. In order to evaluate the effect of impairments present in one side (transmit/receive), the impairment value on the other side (receive/transmit) is set to be zero. It can be observed that at higher SNR values, the effect of δ_r is more severe than that of δ_t and this severity increases as the value of the corresponding impairment increases.

⁹The impairment values of 0.08 or 0.15 are selected based on the required Error Vector Magnitude (EVM) at the transmit-side RF of the LTE system [41, Sec. 14.3.4] and we assume that RF distortion at the receive-side is similar to the transmit-side RF distortion [30].

In order to illustrate the effect of the number of scatterers, we plot per-antenna ergodic capacity versus K in Fig. 3 considering $\rho = 20$ dB, $M = 4$, $N = 5$. It can be noted that the per-antenna ergodic capacity first increases with the value of K and then tends to saturate after a certain value. Moreover, the per-antenna capacity versus K decreases with the increase in the severity of the impairments. Also, the saturation with the variation in K occurs earlier for the higher value of impairments. Herein, we observe a known effect taking place in MIMO channels. More specifically, please note that the capacity increases with K until $K = N = 5$. Then, the saturation tends to start. The reason behind this is by increasing the number of receive antennas N , the amount of received power is increased, but if we increase the number of transmit antennas in the second MIMO product, the power is split between all transmit antennas, and the power instead of increasing, it saturates.

B. High-SNR Analysis

Due to the complexity of (14) describing the ergodic capacity, we perform a high-SNR analysis to provide further insights on the impact of the residual additive transceiver imperfections on the achievable capacity in that regime.

In particular, the high-SNR region is characterized by the affine expansion [42]

$$C(\rho, M, N, K, \delta_t, \delta_r) = \mathcal{S}_\infty \left(\frac{\rho|_{\text{dB}}}{3\text{dB}} - \mathcal{L}_\infty \right) + o(1), \quad (18)$$

where the two relevant parameters

$$\mathcal{S}_\infty = \lim_{\rho \rightarrow \infty} \frac{C(\rho, M, N, K, \delta_t, \delta_r)}{\log_2 \rho} \quad (19)$$

and

$$\mathcal{L}_\infty = \lim_{\rho \rightarrow \infty} \left(\log_2 \rho - \frac{C(\rho, M, N, K, \delta_t, \delta_r)}{\mathcal{S}_\infty} \right) \quad (20)$$

denote the high-SNR slope in bits/s/Hz/(3 dB) and the high-SNR offset in 3 dB units, respectively. Note that 3 dB = $10 \log_{10} 2$.

Proposition 2: In the high-SNR regime ($\rho \rightarrow \infty$), the slope \mathcal{S}_∞ and power offset \mathcal{L}_∞ of Rayleigh-product channels with optimal receivers, accounting for residual additive hardware transceiver impairments are given by

$$\mathcal{S}_\infty = 0 \text{ bits/s/Hz (3 dB)}, \quad (21)$$

and

$$\mathcal{L}_\infty = \mathbb{E} \left[\log_2 \det \left(\frac{\frac{1}{M} \tilde{\delta}_t^2 \mathbf{W} + \delta_r^2 \mathbf{I}_s}{\frac{1}{M} \delta_t^2 \mathbf{W} + \delta_r^2 \mathbf{I}_s} \right) \right], \quad (22)$$

where

$$\mathbf{W} = \frac{1}{K} \begin{cases} \mathbf{H}_2^H \mathbf{H}_1^H \mathbf{H}_1 \mathbf{H}_2 & \text{if } s = M \\ \mathbf{H}_1^H \mathbf{H}_1 \mathbf{H}_2 \mathbf{H}_2^H & \text{if } s = K \\ \mathbf{H}_1 \mathbf{H}_2 \mathbf{H}_2^H \mathbf{H}_1^H & \text{if } s = N, \end{cases} \quad (23)$$

Proof: See Appendix C. ■

Clearly, the high-SNR slope is zero, i.e., the capacity of optimal receivers increases unsaturated. In most cases, this constant depends on the number of scatterers, since this number is the smallest one among M , K , N in Rayleigh-product MIMO channels.

C. Low-SNR Analysis

In the regime of low-SNR, the study of the capacity in terms of $\frac{E_b}{N_0}$ is preferable than the per-symbol SNR, ρ . In particular, the capacity in this region is well approximated according to [43] by

$$C^{\text{opt}} \left(\frac{E_b}{N_0} \right) \approx S_0^{\text{opt}} \log_2 \left(\frac{\frac{E_b^{\text{opt}}}{N_0}}{\frac{E_b}{N_{0\min}}} \right), \quad (24)$$

where the two involved parameters $\frac{E_b^{\text{opt}}}{N_{0\min}}$ and S_0^{opt} represent the minimum transmit energy per information bit and the wideband slope, respectively. Interestingly, we can express them in terms of the first and second derivatives of $C^{\text{opt}}(\rho)$ as

$$\frac{E_b^{\text{opt}}}{N_{0\min}} = \lim_{\rho \rightarrow 0} \frac{\rho}{C^{\text{opt}}(\rho)} = \frac{1}{\dot{C}^{\text{opt}}(0)}, \quad (25)$$

$$S_0^{\text{opt}} = -\frac{2 \left[\dot{C}^{\text{opt}}(0) \right]^2}{\ddot{C}^{\text{opt}}(0)} \ln 2. \quad (26)$$

According to [44], the low-SNR analysis in terms of the wideband slope can illustrate : i) how the low spectral efficiency values are obtained, when a given data rate (b/s) is transmitted through a very large bandwidth. Note that large bandwidth transmission, known also as millimeter-wave transmission, is an emerging technology for the future 5G systems. Hence, the study of the wideband slope is quite informative. A scenario includes the case where a given bandwidth is used to transmit a very small data rate. As a result, the ‘‘wideband regime’’ is to be understood as encompassing any scenario where the number of information bits transmitted per receive dimension is small.

Proposition 3: In the low-SNR regime ($\rho \rightarrow 0$), the minimum transmit energy per information bit $\frac{E_b^{\text{opt}}}{N_{0\min}}$ and the wideband slope S_0^{opt} of Rayleigh-product channels with optimal receivers, accounting for residual additive hardware transceiver impairments, are given by

$$\frac{E_b^{\text{opt}}}{N_{0\min}} = \frac{\ln 2}{N} \quad (27)$$

and

$$S_0^{\text{opt}} = \frac{2KMN}{(1 + 2\delta_t^2)(1 + MN + K(M + N)) + 2KM\delta_r^2}. \quad (28)$$

Proof: See Appendix D. ■

$\frac{E_b^{\text{opt}}}{N_{0\min}}$ denotes the minimum normalized energy per information bit required to convey any positive rate reliably. Interestingly, as in [28], the minimum transmit energy per information bit $\frac{E_b^{\text{opt}}}{N_{0\min}}$ does not depend on the channel impairments. Actually, $\frac{E_b^{\text{opt}}}{N_{0\min}}$ coincides with its value in the ideal case of no hardware impairments, i.e., it is inversely proportional to the number of receive antennas, and is independent of the number of transmit antennas and the number of scatterers. However, the wideband slope decreases with hardware impairments, i.e., the number of information bits transmitted per receive dimension reduces.

IV. ERGODIC SUM-RATE ANALYSIS OF MMSE RECEIVERS

This is the main section, where the ergodic sum-rate with MMSE receivers, is obtained under the practical consideration of additive hardware impairments. Although the probability density function (PDF) of the SINR with MMSE receiver is not available, we follow an approach similar to [14], [45] to obtain the exact expression for the rate corresponding to the optimal receiver.

More concretely, in the case of recovery of the signal \mathbf{x} after multiplication of the received signal \mathbf{y} with a linear filter, the instantaneous received SINR changes depending on the type of the filter. Henceforth, our study focuses on the impact of the residual RF transceiver impairments in the case that the linear MMSE receiver, having the form

$$\mathbf{W} = \sqrt{\frac{M}{\rho}} \mathbf{R}_g^{-1} \mathbf{H}^H, \quad (29)$$

is applied. Note that \mathbf{R}_g is given by

$$\mathbf{R}_g = \mathbf{H}^H \mathbf{H} + \delta_t^2 \mathbf{H}^H \mathbf{H} + M (\delta_r^2 + \rho^{-1}) \mathbf{I}_M. \quad (30)$$

We proceed with the presentation of the corresponding SINR by following a similar procedure to [46]. Hence, the instantaneous received SINR for the m th MMSE receiver element in the presence of residual additive hardware impairments can be written as

$$\gamma_m^{\text{MMSE}} = \frac{1}{\left[(\mathbf{I}_M + \frac{\rho}{M} \mathbf{H}^H \Phi^{-1} \mathbf{H})^{-1} \right]_{m,m}} - 1. \quad (31)$$

Taking into account for independent decoding across the filter outputs, the ergodic sum-rate of the system with MMSE receiver is expressed by

$$C^{\text{MMSE}}(\rho, M, N, K, \delta_t, \delta_r) = \sum_{i=1}^M \mathbb{E} \gamma_i \left\{ \log_2 (1 + \gamma_i^{\text{MMSE}}) \right\}. \quad (32)$$

A. Exact Expression

Theorem 2: The ergodic achievable sum-rate of practical Rayleigh-product channels with MMSE receivers, accounting for residual additive hardware transceiver impairments, reads as

$$C^{\text{MMSE}}(\rho, M, N, K, \delta_t, \delta_r) = MC^{\text{opt}}(\rho, M, N, K, \delta_t, \delta_r) - MC^{\text{opt}}\left(\frac{M-1}{M}\rho, M-1, N, K, \delta_t, \sqrt{\frac{M}{M-1}}\delta_r\right), \quad (33)$$

where $C^{\text{opt}}(\rho, M, N, K, \delta_t, \delta_r)$ is given by (12).

Proof: See Appendix E. ■

Remark 2: The resemblance of Theorem 2 with [14, Theorem 1] is noteworthy, however the current Theorem is more general, since it includes the effects of the residual transceiver impairments by means of δ_t and δ_r . When $\delta_t = \delta_r = 0$, i.e., in the case of no hardware impairments, (33) coincides with Theorem 1 in [14].

In Fig. 4, we compare the per-antenna ergodic achievable sum-rate of Rayleigh-product channels with MMSE receivers

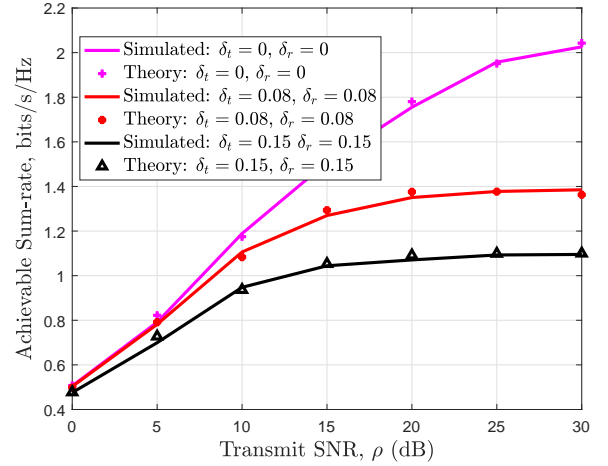


Fig. 4. Per-antenna achievable sum-rate of Rayleigh product channels with MMSE receivers ($K = 3$, $M = 4$, $N = 5$).

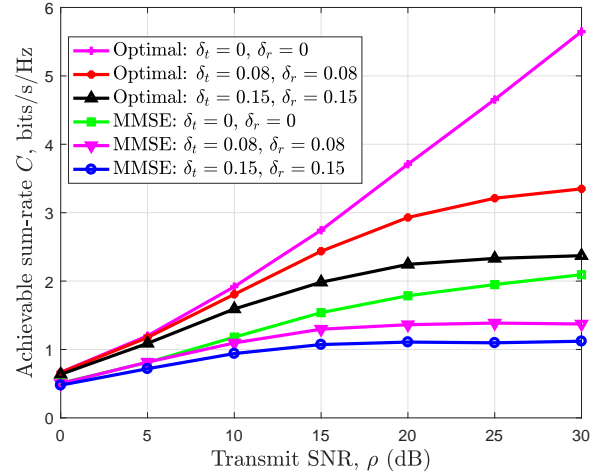


Fig. 5. Comparison between optimal and MMSE receivers in Rayleigh product channels with parameters ($K = 3$, $M = 4$, $N = 5$).

assuming $K = 3$, $M = 4$, $N = 5$. As for the case of optimal receivers in Fig. 2, we demonstrate the perfect agreement between the analytical and the simulated results. The theoretical curves with residual hardware impairments were obtained by evaluating (33) in Theorem 2. It can be depicted from Fig. 4 that the per-antenna ergodic rate of MMSE receivers decreases with the increase in the severity of the impairments. Another observation is that the rate curves with the residual hardware impairments saturate after a certain value of ρ . In order to provide insights on the differences of optimal receiver and MMSE receivers, we also provide the comparison between MMSE and optimal receivers in Fig. 5 considering both the cases with and without the impairments. As expected, the performance of MMSE receivers is less than the performance of the optimal for all the considered cases.

B. High-SNR Analysis

Proposition 4: In the high-SNR regime ($\rho \rightarrow \infty$), the slope S_∞ and the power offset \mathcal{L}_∞ of Rayleigh-product channels with MMSE receivers, accounting for residual additive hard-

ware transceiver impairments are given by

$$\mathcal{S}_\infty = \begin{cases} s \text{ bits/s/Hz (3 dB)} & \text{if } M = s \\ 0 & \text{if } M > s, \end{cases} \quad (34)$$

$$\mathcal{L}_\infty = \begin{cases} (s-1)\mathbb{E}\left[\log_2 \det\left(\frac{\frac{1}{s}\delta_t^2\mathbf{W} + \delta_r^2\mathbf{I}_s}{\frac{1}{s}\delta_t^2\mathbf{W} + \delta_r^2\mathbf{I}_s}\right)\right] & \text{if } M = s \\ \infty & \text{if } M > s \end{cases}. \quad (35)$$

Proof: See Appendix F. ■

Proposition 5 indicates that the high-SNR slope equals to M only if M is smaller than K and N . However, given that we assume a rank deficient channel, the high-SNR slope becomes 0. The same result occurs when the number of receive antennas is insufficient. The reason behind this is the prevention of the perfect cancellation of the co-channel interference. The channel becomes interference-limited and the SINR saturates at high SNR, i.e., the achievable rate does not scale with the SNR.

C. Low-SNR Analysis

The characterization of the minimum transmit energy per information bit and the wideband slope, when MMSE receivers are employed with transceiver hardware impairments, takes place in this section.

Proposition 5: In the low-SNR regime ($\rho \rightarrow 0$), the minimum transmit energy per information bit $\frac{E_b^{\text{MMSE}}}{N_{0\text{min}}}$ and the wideband slope S_0^{MMSE} of Rayleigh-product channels with MMSE receivers, accounting for residual additive hardware transceiver impairments are given by

$$\frac{E_b^{\text{MMSE}}}{N_{0\text{min}}} = \frac{\ln 2}{N} \quad (36)$$

and

$$S_0^{\text{MMSE}} = \frac{2KMN}{(2KM\delta_r^2 + ((2M-1)(N+K) + KN + 1)(1 + \delta_t^2)) (1 + \delta_t^2)}. \quad (37)$$

Proof: See Appendix G. ■

Remark 3: Increasing the transmit hardware impairment, $\frac{E_b^{\text{MMSE}}}{N_{0\text{min}}}$ increases. Moreover, the wideband slope depends on both transmit and receive impairments. In fact, when the quality of the transceiver hardware becomes worse, the wideband slope decreases.

Figs. 6 and 7 illustrate the per-antenna ergodic capacity and the achievable sum-rate versus E_b/N_0 for optimal and MMSE receivers, respectively. The results for optimal receivers were plotted by following the low-SNR analysis presented in Section III-C. Similarly, for the case of MMSE receivers, the low-SNR analysis presented above was taken into account. It can be noted for the case of optimal receivers, all curves with and without impairments converge at the minimum E_b/N_0 value, i.e., $E_b/N_{0\text{min}}$. The capacity gap with respect to the case without impairments increases with the increase in the value of E_b/N_0 by means of an increase of the wideband slope as lower quality transceiver hardware is used.

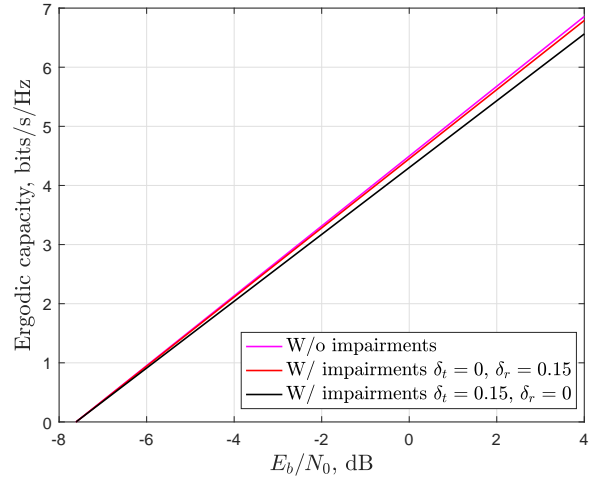


Fig. 6. Per-antenna ergodic capacity versus E_b/N_0 for optimal receivers.

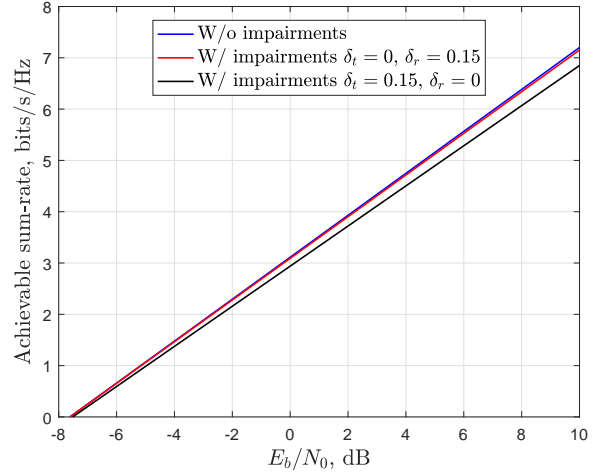


Fig. 7. Per-antenna achievable sum-rate versus E_b/N_0 for MMSE receivers.

V. ASYMPTOTIC SUM-RATE ANALYSIS OF OPTIMAL LINEAR RECEIVERS

In this section, we provide the asymptotic analysis in the presence of residual additive transceiver impairments for the ergodic capacity and the achievable sum-rate of Rayleigh-product MIMO channels with optimal receivers. Employing tools from large RMT, and in particular, conducting a free probability analysis [1], [22], [23], we shed light on the effect of hardware imperfections on large MIMO deployments. Contrary to existing literature that usually employs a deterministic equivalent analysis, we use FP because it requires just a polynomial solution instead of fixed-point equations, and allows us to provide a thorough characterization of the impact of the residual transceiver impairments on the performance of Rayleigh-product MIMO channels in the large antenna limit.

The following variable definitions allow us to simplify the analysis. Specifically, we denote

$$\tilde{\mathbf{N}}_1 = \mathbf{H}_1^H \mathbf{H}_1 \quad (38)$$

$$\tilde{\mathbf{N}}_2 = \mathbf{H}_2 \mathbf{H}_2^H \quad (39)$$

$$\mathbf{K} = \tilde{\mathbf{N}}_2 \tilde{\mathbf{N}}_1, \quad (40)$$

where the number of transmit and receive antennas (M and N) as well as the number of scatterers K tend to infinity with given ratios $\beta = \frac{M}{K}$ and $\gamma = \frac{K}{N}$. Note that the study of the Rayleigh-product does not mean necessarily that K must be small. However, since we examine a rank deficient channel, where $M > K$, we have $s = K$.

Letting the system dimensions tend to infinity while keeping their finite ratios β and γ fixed, we can obtain the asymptotic limit of the capacity per receive antenna, if we divide it by N and write (12) as

$$\tilde{C}^{\text{opt}}(\rho, \beta, \gamma, \delta_t, \delta_r) = \tilde{C}_1^{\text{opt}}(\rho, \beta, \gamma, \delta_t, \delta_r) - \tilde{C}_2^{\text{opt}}(\rho, \beta, \gamma, \delta_t, \delta_r), \quad (41)$$

where \tilde{C}_i^{opt} for $i = 1, 2$ is expressed as

$$\begin{aligned} \tilde{C}_i^{\text{opt}} &= \frac{1}{N} \lim_{K, M, N \rightarrow \infty} \mathbb{E}[\log_2 \det(\mathbf{I}_K + f_i \mathbf{H}_2 \mathbf{H}_2^H \mathbf{H}_1^H \mathbf{H}_1)] \\ &= \frac{K}{N} \lim_{K, M, N \rightarrow \infty} \mathbb{E} \left[\frac{1}{K} \sum_{j=1}^K \log_2 \left(1 + f_i K \lambda_j \left(\frac{1}{K} \mathbf{K} \right) \right) \right] \\ &\rightarrow \gamma \int_0^\infty \log_2(1 + f_i K x) f_{\frac{K}{K}}^\infty(x) dx. \end{aligned} \quad (42)$$

Note that $\lambda_j(\frac{1}{K}\mathbf{K})$ is the j th ordered eigenvalue of matrix $\frac{1}{K}\mathbf{K}$, and $f_{\frac{1}{K}\mathbf{K}}^\infty$ denotes the asymptotic eigenvalue probability density function (a.e.p.d.f.) of $\frac{1}{K}\mathbf{K}$. In the asymptotic numbers of antennas and scatterers limit, the per receive antenna ergodic capacity of Rayleigh-product MIMO channels with residual transceiver hardware impairments, is provided by the following theorem¹⁰.

Theorem 3: The per receive antenna ergodic capacity of Rayleigh-product MIMO channels for optimal receivers in the presence of additive transceiver impairments, when the number of transmit and receive antennas (M and N) as well as the number of scatterers K tend to infinity with given ratios β and γ , is given by

$$\tilde{C}^{\text{opt}}(\rho, \beta, \gamma, \delta_t, \delta_r) \rightarrow \gamma \int_0^\infty \log_2 \left(\frac{1 + f_1 K x}{1 + f_2 K x} \right) f_{\frac{K}{K}}^\infty(x) dx, \quad (43)$$

where $\tilde{C}^{\text{opt}} = C^{\text{opt}}/N$ is the per receive antenna ergodic capacity, while the a.e.p.d.f. of $\frac{K}{K} f_{\frac{K}{K}}^\infty$ is obtained by finding the imaginary part of its Stieltjes transform \mathcal{S} for real arguments.

Proof: See Appendix H. ■

In order to validate our asymptotic analysis of the ergodic capacity of optimal linear receivers presented in Subsection IV.A, we plot the a.e.p.d.f. of \mathbf{K} in Fig. 8, where the histogram represents the p.d.f. of the matrix \mathbf{K} calculated numerically based on MC simulations. Furthermore, the solid line depicts the a.e.p.d.f. obtained by solving the polynomial (78) of the Stieltjes transform of the corresponding a.e.p.d.f., and then applying Lemma 3. A perfect agreement between the results obtained from theoretical analysis and MC simulations has been obtained, as reflected in Fig. 8.

¹⁰For the achievable rate of MMSE receivers in the asymptotic regime, starting with (31), one can find the polynomial for the Stieltjes transform of the involved matrix term following the procedure in [47], then find the corresponding asymptotic eigenvalue probability density function and then derive the asymptotic capacity expression as done for the case of optimal receivers.

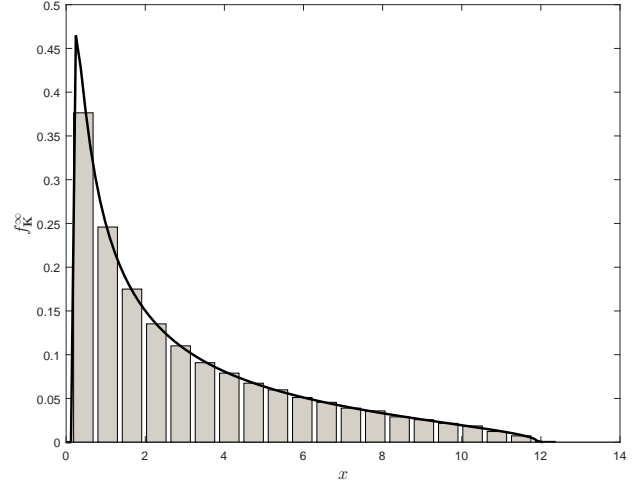


Fig. 8. A.e.p.d.f. of \mathbf{K} ($\rho = 20$ dB, $K = 100$, $M = 300$, $N = 200$, $\delta_t = \delta_r = 0.15$).

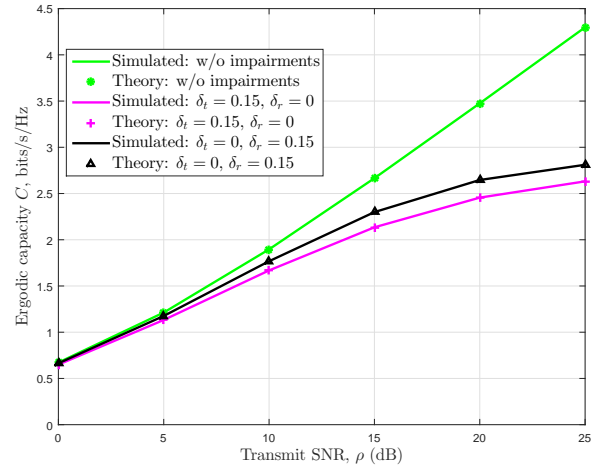


Fig. 9. Asymptotic per-antenna ergodic capacity versus ρ ($K = 100$, $M = 300$, $N = 200$).

In Fig. 9, we plot the theoretical and simulated per-antenna ergodic capacities versus ρ considering $K = 100$, $M = 300$, and $N = 200$. Both the cases with and without impairments are presented. From the figure, it can be observed that theoretical and simulated capacity curves for both the considered cases match perfectly. Moreover, as expected, the per-antenna capacity increases with the increase in the value of ρ in the absence of impairments, i.e., $\delta_t = \delta_r = 0$. However, as in the finite case, the per-antenna capacity tends to saturate after a certain value of ρ in the presence of impairments.

Fig. 10 depicts the per-antenna capacity versus β and γ by considering parameters ($K = 10$, $\rho = 20$ dB, $\delta_t = 0.15$, $\delta_r = 0.15$). It can be noted that the per-antenna capacity increases with the increase in the value of $\gamma = \frac{K}{N}$ but decreases with the value of $\beta = \frac{M}{K}$ over the considered range. Another important observation is that the rate of capacity variation with respect to β is much steeper than the capacity variation with γ .

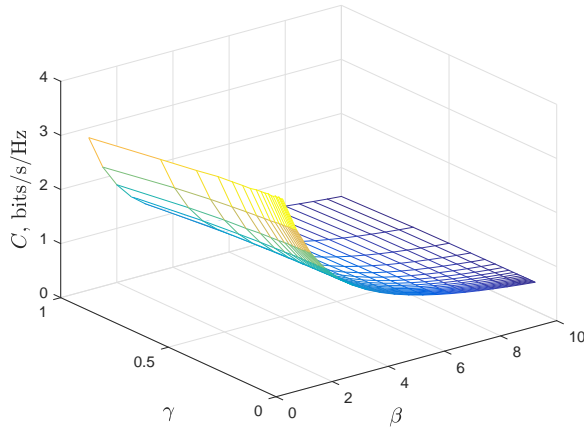


Fig. 10. Asymptotic per-antenna ergodic capacity versus β and γ for optimal receivers ($K = 10$, $\rho = 20$ dB, $\delta_t = 0.15$, $\delta_r = 0.15$).

VI. CONCLUSIONS

In this paper, we provided an exact characterization of the performance of double Rayleigh MIMO channels in the presence of residual transceiver hardware impairments. In particular, it was noted that the per-antenna ergodic capacity with optimal receivers first increases with the SNR and then gets saturated after a certain value of the SNR. The same behaviour of the ergodic capacity was observed with the increase in the number of scatterers. Furthermore, it was demonstrated that the ergodic capacity decreases with the increase in the severity of the impairments. Also, it was observed that the effect of severity of transmit-side and receive-side impairments in the considered Rayleigh-Product MIMO system depends on the operating SNR region as well as the finite or asymptotic regimes of the considered system dimensions. Similar observations hold for the achievable sum-rate with MMSE receivers. Notably, the minimum transmit energy per information bit for optimal and MMSE receivers is independent on the additive impairments. Moreover, we demonstrated the behavior of double Rayleigh MIMO channels for optimal receivers, when the number of antennas and scatterers is large. In our future work, we plan to extend our analysis for the case of multiplicative transceiver impairments.

APPENDIX A USEFUL LEMMAS

Herein, given the eigenvalue probability distribution function $f_{\mathbf{X}}(x)$ of a matrix \mathbf{X} , we provide useful definitions and lemmas that are considered during our analysis. In the following definitions, δ is a nonnegative real number.

Definition 1 (η -transform [48, Definition 2.11]): The η -transform of a positive semidefinite matrix \mathbf{X} is defined as

$$\eta_{\mathbf{X}}(\delta) = \int_0^{\infty} \frac{1}{1 + \delta x} f_{\mathbf{X}}(x) dx. \quad (44)$$

Definition 2: [S-transform [48, Definition 2.15]] The S-transform of a positive semidefinite matrix \mathbf{X} is defined as

$$\Sigma_{\mathbf{X}}(x) = -\frac{x+1}{x} \eta_{\mathbf{X}}^{-1}(x+1). \quad (45)$$

Lemma 1 ([48, Eqs. 2.87, 2.88]): Given a Gaussian $K \times M$ channel matrix $\mathbf{H} \sim \mathcal{CN}(\mathbf{0}, \mathbf{I})$, the S-transform of the matrix $\frac{1}{K} \mathbf{H}^H \mathbf{H}$ is expressed as

$$\Sigma_{\frac{1}{K} \mathbf{H}^H \mathbf{H}}(x, \beta) = \frac{1}{1 + \beta x}, \quad (46)$$

while the S-transform of the matrix $\frac{1}{K} \mathbf{H} \mathbf{H}^H$ is obtained as

$$\Sigma_{\frac{1}{K} \mathbf{H} \mathbf{H}^H}(x, \beta) = \frac{1}{\beta + x}, \quad (47)$$

Lemma 2 ([48, Eq. 2.48]): The Stieltjes-transform of a positive semidefinite matrix \mathbf{X} can be derived by its η -transform according to

$$\mathcal{S}_{\mathbf{X}}(x) = -\frac{\eta_{\mathbf{X}}(-1/x)}{x}. \quad (48)$$

Lemma 3 ([48, Eq. 2.45]): The asymptotic eigenvalue probability density function (a.e.p.d.f.) of \mathbf{X} is obtained by the imaginary part of the Stieltjes transform \mathcal{S} for real arguments as

$$f_{\mathbf{X}}^{\infty}(x) = \lim_{y \rightarrow 0^+} \frac{1}{\pi} \Im \{ \mathcal{S}_{\mathbf{X}}(x + jy) \}. \quad (49)$$

APPENDIX B PROOF OF THEOREM 1

Proof: First, we denote

$$\mathbf{W} = \frac{1}{K} \begin{cases} \mathbf{H}_2^H \mathbf{H}_1^H \mathbf{H}_1 \mathbf{H}_2 & \text{if } s = M \\ \mathbf{H}_1^H \mathbf{H}_1 \mathbf{H}_2 \mathbf{H}_2^H & \text{if } s = K \\ \mathbf{H}_1 \mathbf{H}_2 \mathbf{H}_2^H \mathbf{H}_1^H & \text{if } s = N, \end{cases} \quad (50)$$

where $\mathbf{H}_1, \mathbf{H}_2$ are given by (2). We employ Corollary 2 in [49] providing the PDF of an unordered eigenvalue $p(\lambda)$ of the matrix $\mathbf{H}_2^H \mathbf{H}_1^H \mathbf{H}_1 \mathbf{H}_2$, in order to write (12) in terms of the eigenvalues of \mathbf{W} . Especially, $p(\lambda)$ is read as

$$p(\lambda) = 2\mathcal{K} \sum_{i=1}^s \sum_{j=1}^s \frac{\lambda^{\frac{p+2j+t+i-2s-3}{2}} K_{t-p+i-1}(2\sqrt{\lambda}) G_{i,j}}{s\Gamma(p-s+j)}, \quad (51)$$

where \mathcal{K} is given by (16), and $K_\nu(x)$ is the modified Bessel function of the second kind [38, eq. 8.432.1]. Hence, we have from (12)

$$C^{\text{opt}}(\rho, M, N, K, \delta_t, \delta_r) = s \int_0^{\infty} \log_2 \left(1 + \frac{\frac{\rho}{KM} \lambda}{\frac{\rho \delta_t^2 \lambda}{KM} + \rho \delta_r^2 + 1} \right) p(\lambda) d\lambda \quad (52)$$

$$= s \int_0^{\infty} \log_2 \left((1 + \delta_t^2) \frac{\rho \lambda}{KM} + \rho \delta_r^2 + 1 \right) p(\lambda) d\lambda \\ - s \int_0^{\infty} \log_2 \left(\frac{\rho}{KM} \delta_t^2 \lambda + \rho \delta_r^2 + 1 \right) p(\lambda) d\lambda. \quad (53)$$

Substitution of (51) into (53) and making use of [38, eq. 7.821.3] after expressing the logarithm in terms of a Meijer G-function according to $\ln(1+x) = G_{2,2}^{1,2}(ax | \begin{smallmatrix} 1,1 \\ 0,0 \end{smallmatrix})$ [50, eq. 8.4.6.5] concludes the proof. \blacksquare

APPENDIX C
PROOF OF PROPOSITION 2

First, we write (12) as

$$\begin{aligned} C^{\text{opt}}(\rho, M, N, K, \delta_t, \delta_r) &= \mathbb{E} \left[\log_2 \det \left(\Phi + \frac{\rho}{M} \mathbf{W} \right) - \log_2 \det(\Phi) \right] \\ &= \mathbb{E} \left[\log_2 \det \left((1 + \delta_t^2) \frac{\rho}{M} \mathbf{W} + (\delta_r^2 \rho + 1) \mathbf{I}_s \right) \right] \end{aligned} \quad (54)$$

$$\begin{aligned} &- \log_2 \det \left(\frac{\rho}{KM} \delta_t^2 \mathbf{W} + (\delta_r^2 \rho + 1) \mathbf{I}_s \right) \\ &= \mathbb{E} \left[\log_2 \det \left(\frac{\frac{1}{M}(1 + \delta_t^2) \mathbf{W} + \left(\delta_r^2 + \frac{1}{\rho} \right) \mathbf{I}_s}{\frac{1}{M} \delta_t^2 \mathbf{W} + \left(\delta_r^2 + \frac{1}{\rho} \right) \mathbf{I}_s} \right) \right]. \end{aligned} \quad (55)$$

Note that in (54) we have considered that \mathbf{W} , given by (50), has s non-zero eigenvalues. Applying to (55) the definition of the high-SNR slope, provided by (19), we obtain

$$\mathcal{S}_\infty^{\text{opt}} = 0. \quad (56)$$

The high-SNR offset, defined by (20), can be derived by appropriate substitution of (55). As a result, \mathcal{L}_∞ reads as

$$\mathcal{L}_\infty = \mathbb{E} \left[\log_2 \det \left(\frac{(1 + \delta_t^2) \frac{1}{M} \mathbf{W} + \delta_r^2 \mathbf{I}_s}{\frac{1}{M} \delta_t^2 \mathbf{W} + \delta_r^2 \mathbf{I}_s} \right) \right]. \quad (57)$$

APPENDIX D
PROOF OF PROPOSITION 3

In order to obtain $\frac{E_b}{N_{0\min}}$ and S_0 , we need to derive the first and second derivatives of the ergodic capacity. The two following useful lemmas generalize [44, Eqs. 210 and 211], when \mathbf{A} depends on ρ , and $f(\rho)$ does not equal just to ρ , but it is a general function regarding this variable.

Lemma 4:

$$\begin{aligned} &\frac{\partial}{\partial \rho} \ln \det (\mathbf{I} + f(\rho) \mathbf{A}(\rho)) \Big|_{\rho=0} \\ &= \text{tr} \left((\mathbf{I} + f(0) \mathbf{A}(0))^{-1} \left(f'(0) \mathbf{A}(0) + f(0) \mathbf{A}'(0) \right) \right). \end{aligned} \quad (58)$$

Proof: First, we obtain the derivative of the first part of (58) with respect to ρ as

$$\frac{\partial}{\partial \rho} \ln \det \mathbf{G}(\rho) = \frac{\frac{\partial \det \mathbf{G}(\rho)}{\partial \rho}}{\det \mathbf{G}(\rho)} \quad (59)$$

$$= \text{tr} \left(\mathbf{G}^{-1}(\rho) \frac{\partial \mathbf{G}(\rho)}{\partial \rho} \right), \quad (60)$$

where we have denoted $\mathbf{G}(\rho) = \mathbf{I} + f(\rho) \mathbf{A}(\rho)$, and we have applied [51, Eq. 46]. Note that

$$\frac{\partial \mathbf{G}(\rho)}{\partial \rho} = f'(\rho) \mathbf{A}(\rho) + f(\rho) \mathbf{A}'(\rho). \quad (61)$$

By substituting (61) into (60), and letting $\rho = 0$, we lead to (58). ■

Lemma 5:

$$\frac{\partial^2}{\partial \rho^2} \ln \det \mathbf{G}(0) = \text{tr} \left(\mathbf{G}^{-1}(0) \left(\frac{\partial^2 \mathbf{G}(0)}{\partial \rho^2} - \left(\frac{\partial \mathbf{G}(0)}{\partial \rho} \right)^2 \right) \right), \quad (62)$$

where $\mathbf{G}'(0)$ and $\mathbf{G}''(0)$ are obtained by setting $\rho = 0$ to (61) and (64), respectively.

Proof: Obtaining the second derivative of $\ln \mathbf{G}(\rho)$ by (59), we have

$$\frac{\partial^2}{\partial \rho^2} \ln \det \mathbf{G}(\rho) = \text{tr} \left(\mathbf{G}^{-1}(\rho) \left(\frac{\partial^2 \mathbf{G}(\rho)}{\partial \rho^2} - \left(\frac{\partial \mathbf{G}(\rho)}{\partial \rho} \right)^2 \right) \right), \quad (63)$$

where we have used [51, Eq. 48]. The first derivative of \mathbf{G} is given by (61), while the second derivative is obtained after following a similar procedure to Lemma 4 as

$$\frac{\partial^2 \mathbf{G}(\rho)}{\partial \rho^2} = f''(\rho) \mathbf{A}(\rho) + 2f'(\rho) \mathbf{A}'(\rho) + f(\rho) \mathbf{A}''(\rho). \quad (64)$$

Appropriate substitutions of (64) and (61) into (63) and simple algebraic manipulations provide the desired result after setting $\rho = 0$. ■

Herein, having denoted $C^{\text{opt}}(\rho, M, N, K, \delta_t, \delta_r)$ as in (53), we can write for $i = 1, 2$ that

$$C_i(\rho, M, N, K, \delta_t, \delta_r) = \mathbb{E} [\log_2 \det (f_i(\rho) \mathbf{F} + \mathbf{I}_s)]. \quad (65)$$

We assume that \mathbf{F} plays the role of \mathbf{A} in Lemmas 4, 5, while $f_1(\rho) = \frac{\rho}{KM} \frac{(1 + \delta_t^2)}{\rho \delta_t^2 + 1}$ and $f_2(\rho) = \frac{\rho}{KM} \frac{\delta_t^2}{\rho \delta_t^2 + 1}$. When $\rho \rightarrow 0$, we find that $f_1(0) = f_2(0) = 0$, while its first and second derivatives at $\rho = 0$ equal to $f_1'(0) = \frac{\delta_t^2}{KM}$, $f_2'(0) = \frac{\delta_t^2}{KM}$, and $f_1''(0) = -\frac{2\delta_t^2 \delta_t^2}{KM}$, $f_2''(0) = -\frac{2\delta_t^2 \delta_t^2}{KM}$. Thus, using the fact that $\mathbf{G}_i(\rho) = \mathbf{I} + f_i(\rho) \mathbf{F}(\rho)$, we have $\mathbf{G}_i(0) = \mathbf{I}_N$. By taking the first derivative of (53), and applying Lemma 4, we have

$$\begin{aligned} \dot{C}^{\text{opt}}(0) &= \frac{1}{\ln 2} \frac{\partial}{\partial \rho} \mathbb{E} [\ln \det \mathbf{G}(\rho)] \Big|_{\rho=0} \\ &= \frac{(f_1'(0) - f_2'(0))}{\ln 2} \mathbb{E} [\text{tr} \mathbf{F}] \\ &= \frac{N}{\ln 2}, \end{aligned} \quad (66)$$

since $\mathbb{E} [\text{tr} \mathbf{F}] = KMN$. Similarly, the second derivative of C^{opt} at $\rho = 0$ can be written by means of Lemma (5) as

$$\begin{aligned} \ddot{C}^{\text{opt}}(0) &= \frac{1}{\ln 2} \frac{\partial^2}{\partial \rho^2} \mathbb{E} [\ln \det \mathbf{G}(\rho)] \Big|_{\rho=0} \\ &= \frac{(f_1''(0) - f_2''(0))}{\ln 2} \mathbb{E} [\text{tr} \mathbf{F}] - \frac{\left((f_1'(0))^2 - (f_2'(0))^2 \right)}{\ln 2} \mathbb{E} [\text{tr} \mathbf{F}^2] \\ &= -\frac{\left((1 + 2\delta_t^2)(1 + MN + K(M + N)) + 2KM\delta_t^2 \right) N}{KM \ln 2}, \end{aligned} \quad (67)$$

where $\mathbb{E} [\text{tr} \mathbf{F}^2] = M^2KN(K + N) + MKN(NK + 1)$ by taking advantage of [52, Theorem 7]. Appropriate substitutions and algebraic manipulations of (66) and (67), enable us to obtain first $\frac{E_b}{N_{0\min}}$ by means of (25), and in turn, S_0 by means of (26).

APPENDIX E
PROOF OF THEOREM 2

We pursue a standard procedure as in [14], [45]. In particular, first, we consider the following property allowing to express the i th diagonal element of an inverse matrix \mathbf{Z}^{-1} with

regards to the determinant of the matrix and its (i, i) th minor \mathbf{Z}^{ii} . Specifically, we have

$$[\mathbf{Z}^{-1}]_{ii} = \frac{\det \mathbf{Z}^{ii}}{\det \mathbf{Z}}. \quad (68)$$

Inserting (31) into (32), and taking into account this property, we obtain

$$\begin{aligned} & C^{\text{MMSE}}(\rho, M, N, K, \delta_t, \delta_r) \\ &= M \mathbb{E} \left[\log_2 \det \left(\mathbf{I}_M + \frac{\rho}{KM} \mathbf{H}_2^H \mathbf{H}_1^H \Phi^{-1} \mathbf{H}_1 \mathbf{H}_2 \right) \right] - \\ & \sum_{i=1}^M \mathbb{E} \left[\log_2 \det \left(\mathbf{I}_{M-1} + \frac{\rho}{KM} (\mathbf{H}_2^H \mathbf{H}_1^H \Phi^{-1} \mathbf{H}_1 \mathbf{H}_2)^{ii} \right) \right]. \end{aligned} \quad (69)$$

The proof is concluded by means of some algebraic manipulations, and by noting that

$$(\mathbf{H}_2^H \mathbf{H}_1^H \mathbf{H}_1 \Phi^{-1} \mathbf{H}_2)^{ii} = \mathbf{H}_{2i}^H \mathbf{H}_1^H \Phi^{-1} \mathbf{H}_1 \mathbf{H}_{2i}, \quad (70)$$

where \mathbf{H}_{2i} is the matrix \mathbf{H}_2 after removing its i th column.

APPENDIX F PROOF OF PROPOSITION 4

Starting from Proposition 2 and following a similar procedure to its proof, we obtain the desired results after several simple algebraic manipulations and by the property of the expansion of a determinant to its minors.

APPENDIX G PROOF OF PROPOSITION 5

Similar to the proof of Proposition 3, the derivation of $\frac{E_b^{\text{MMSE}}}{N_{\text{omin}}}$ and S_0^{MMSE} imposes first the calculation of the first and second derivatives of $C^{\text{MMSE}}(\rho, M, N, K, \delta_t, \delta_r)$ at $\rho = 0$. Taking the first derivative of (33) and using the property in (70), we have

$$\dot{C}^{\text{MMSE}}(\rho, M, N, K, \delta_t, \delta_r) = \frac{N}{(1 + \delta_t^2) \ln 2}. \quad (71)$$

As far as the second derivative of $C^{\text{MMSE}}(\rho, M, N, K, \delta_t, \delta_r)$, we use the same methodology and after several algebraic manipulations, we obtain $\ddot{C}^{\text{MMSE}}(\rho, M, N, K, \delta_t, \delta_r)$ as

$$\begin{aligned} \ddot{C}^{\text{MMSE}}(\rho, M, N, K, \delta_t, \delta_r) &= -\frac{N}{(1 + \delta_t^2)} \\ &\times \left(\frac{((2M-1)(N+K) + KN + 1)(1 + \delta_t^2) + 2KM\delta_r^2}{KM} \right). \end{aligned} \quad (72)$$

After appropriate substitutions, the proof is concluded.

APPENDIX H PROOF OF THEOREM 3

According to the principles of free probability, the a.e.p.d.f. of \mathbf{K}/K can be obtained by means of Lemma 3 that includes its Stieltjes transform $\mathcal{S}_{\mathbf{K}/K}$. Hence, our interest is focused on the derivation of the Stieltjes transform of \mathbf{K}/K . Looking carefully at Lemma 2, we observe that $\mathcal{S}_{\mathbf{K}/K}$ can be obtained by means of its η -transform. Especially, we are going to show

how to acquire the inverse η -transform of \mathbf{K}_α/K . Thus, we obtain the inverse of $\eta_{\mathbf{K}/K}(x)$ by means of this lemma as

$$x\eta_{\mathbf{K}/K}^{-1}(-x\mathcal{S}_{\mathbf{K}/K}(x)) + 1 = 0. \quad (73)$$

In particular, the following proposition provides $\eta_{\mathbf{K}/K}^{-1}(x)$.

Proposition 6: The inverse η -transform of \mathbf{K}/K is given by

$$\eta_{\mathbf{K}/K}^{-1}(x) = -\frac{x-1}{x(\beta+x-1)(\gamma(x-1)+1)}. \quad (74)$$

Proof: Applying the S-transform to (40) and the free convolution we obtain $\eta_{\mathbf{K}/K}^{-1}(x)$ as

$$\Sigma_{\mathbf{K}/K}(x) = \Sigma_{\tilde{\mathbf{N}}_2/K}(x) \Sigma_{\tilde{\mathbf{M}}/K}(x) \iff \quad (75)$$

$$\left(-\frac{x+1}{x} \right) \eta_{\mathbf{K}/K}^{-1}(x+1) = \frac{1}{(\beta+x)(\gamma x+1)},$$

where in (75), we have applied Definition 2 and Lemmas 1, 2. Basically, $\Sigma_{\tilde{\mathbf{N}}_2/K}(x)$ and $\Sigma_{\tilde{\mathbf{N}}_1/K}(x)$ are given by (46) and (47) as

$$\Sigma_{\tilde{\mathbf{N}}_2/K}(x) = \frac{1}{\gamma x + 1} \quad (76)$$

and

$$\Sigma_{\tilde{\mathbf{N}}_1/K}(x) = \frac{1}{\beta + x}. \quad (77)$$

In addition, in (75), we have taken into account the asymptotic freeness between the deterministic matrix with bounded eigenvalues $\tilde{\mathbf{N}}_2$ and the unitarily invariant matrix $\tilde{\mathbf{N}}_1$. Setting $y = x + 1$, i.e., making a change of variables, we obtain (74). ■

Proposition 6 and (73) result after some tedious algebraic manipulations to the following cubic polynomial

$$\begin{aligned} & x^2 \gamma \mathcal{S}_{\mathbf{K}/K}^3 - (\beta \gamma - 2\gamma + 1) x \mathcal{S}_{\mathbf{K}/K}^2 \\ & - (\beta \gamma - \beta - \gamma + x + 1) \mathcal{S}_{\mathbf{K}/K} - 1 = 0, \end{aligned} \quad (78)$$

which provides $\mathcal{S}_{\mathbf{K}/K}$, and thus, $f_{\mathbf{K}/K}^\infty(x)$ by means of (49). This step concludes the proof.

REFERENCES

- [1] A. Papazafeiropoulos, S. K. Sharma, S. Chatzinotas, T. Ratnarajah, and B. Ottersten, "Impact of transceiver hardware impairments on the ergodic channel capacity for Rayleigh-product MIMO channels," in *IEEE Signal Processing Advances in Wireless Communications (SPAWC 2016)*, Edinburgh, U.K., July 2016.
- [2] E. Telatar, "Capacity of multi-antenna Gaussian channels," *Europ. Trans. on Telecom.*, vol. 10, no. 6, pp. 585–595, 1999.
- [3] M. Chiani, M. Z. Win, and A. Zanella, "On the capacity of spatially correlated MIMO rayleigh-fading channels," *IEEE Trans. on Inform. Theory*, vol. 49, no. 10, pp. 2363–2371, 2003.
- [4] S. K. Jayaweera and H. V. Poor, "On the capacity of multiple-antenna systems in Rician fading," *IEEE Trans. on Wireless Commun.*, vol. 4, no. 3, pp. 1102–1111, 2005.
- [5] D. Gesbert, H. Bölcskei, D. A. Gore, and A. J. Paulraj, "Outdoor MIMO wireless channels: Models and performance prediction," *IEEE Trans. on Commun.*, vol. 50, no. 12, pp. 1926–1934, 2002.
- [6] D. Chizhik, G. J. Foschini, M. J. Gans, R. Valenzuela *et al.*, "Keyholes, correlations, and capacities of multielement transmit and receive antennas," *IEEE Trans. on Wireless Commun.*, vol. 1, no. 2, pp. 361–368, 2002.
- [7] D. Shiu, G. J. Foschini, M. J. Gans, and J. M. Kahn, "Fading correlation and its effect on the capacity of multi-element antenna systems," *IEEE Trans. on Commun.*, vol. 48, no. 3, pp. 502–513, 2000.

- [8] J. P. Kermoal, L. Schumacher, K. I. Pedersen, P. E. Mogensen, and F. Frederiksen, "A stochastic MIMO radio channel model with experimental validation," *IEEE Journal on Sel. Areas in Commun.*, vol. 20, no. 6, pp. 1211–1226, 2002.
- [9] P. Almers, F. Tufvesson, and A. F. Molisch, "Measurement of keyhole effect in a wireless multiple-input multiple-output (MIMO) channel," *IEEE Commun. Lett.*, vol. 7, no. 8, pp. 373–375, 2003.
- [10] H. Shin, M. Z. Win, J. H. Lee, and M. Chiani, "On the capacity of doubly correlated MIMO channels," *IEEE Trans. on Wireless Commun.*, vol. 5, no. 8, pp. 2253–2265, 2006.
- [11] R. R. Muller and H. Hofstetter, "Confirmation of random matrix model for the antenna array channel by indoor measurements," in *Proc. IEEE Int. Symp. Antennas and Propagation Society*, vol. 1. IEEE, 2001, pp. 472–475.
- [12] D. Gesbert, H. Bölcskei, D. Gore, A. J. Paulraj *et al.*, "Outdoor MIMO wireless channels: Models and performance prediction," *IEEE Trans. Commun.*, vol. 50, no. 12, pp. 1926–1934, 2002.
- [13] H. Shin and J. H. Lee, "Capacity of multiple-antenna fading channels: Spatial fading correlation, double scattering, and keyhole," *IEEE Trans. on Inform. Theory*, vol. 49, no. 10, pp. 2636–2647, 2003.
- [14] C. Zhong, T. Ratnarajah, Z. Zhang, K. K. Wong, and M. Sellathurai, "Performance of Rayleigh-product MIMO channels with linear receivers," *IEEE Trans. Wireless Commun.*, vol. 13, no. 4, pp. 2270–2281, 2014.
- [15] T. Schenk, *RF imperfections in high-rate wireless systems: impact and digital compensation*. Springer Science & Business Media, 2008.
- [16] C. Studer, M. Wenk, and A. Burg, "MIMO transmission with residual transmit-RF impairments," in *ITG/IEEE Work. Smart Ant. (WSA)*. IEEE, 2010, pp. 189–196.
- [17] J. Qi and S. Aïssa, "On the power amplifier nonlinearity in MIMO transmit beamforming systems," *IEEE Trans. Commun.*, vol. 60, no. 3, pp. 876–887, 2012.
- [18] H. Mehrpouyan, A. Nasir, S. Blostein, T. Eriksson, G. Karagiannidis, and T. Svensson, "Joint estimation of channel and oscillator phase noise in MIMO systems," *IEEE Trans. Signal Processing*, vol. 60, no. 9, pp. 4790–4807, Sept 2012.
- [19] B. Goransson, S. Grant, E. Larsson, and Z. Feng, "Effect of transmitter and receiver impairments on the performance of MIMO in HSDPA," in *IEEE 9th Int. Workshop Signal Process. Adv. Wireless Commun. (SPAWC)*. IEEE, 2008, pp. 496–500.
- [20] J. Qi and S. Aïssa, "Analysis and compensation of I/Q imbalance in MIMO transmit-receive diversity systems," *IEEE Trans. Commun.*, vol. 58, no. 5, pp. 1546–1556, 2010.
- [21] E. Björnson, P. Zetterberg, M. Bengtsson, and B. Ottersten, "Capacity limits and multiplexing gains of MIMO channels with transceiver impairments," *IEEE Commun. Lett.*, vol. 17, no. 1, pp. 91–94, 2013.
- [22] A. Papazafeiropoulos, S. K. Sharma, and S. Chatzinotas, "MMSE filtering performance of DH-AF massive MIMO relay systems with residual transceiver impairments," in *IEEE International Conference on Communications (ICC 2016)*, Kuala Lumpur, Malaysia, May 2016.
- [23] A. Papazafeiropoulos and T. Ratnarajah, "Rate-splitting robustness in multi-pair massive MIMO relay systems," submitted, available upon request, 2017.
- [24] A. K. Papazafeiropoulos, S. K. Sharma, S. Chatzinotas, and B. Ottersten, "Ergodic capacity analysis of AF-DH MIMO relay systems with residual transceiver hardware impairments: Conventional and large system limits," *IEEE Trans. on Veh. Tech.*, vol. 66, no. 8, pp. 7010–7025, Aug 2017.
- [25] A. Papazafeiropoulos and T. Ratnarajah, "Downlink MIMO HCNs with residual transceiver hardware impairments," *IEEE Commun. Letters*, 2016.
- [26] —, "Towards a realistic assessment of multiple antenna HCNs: Residual additive transceiver hardware impairments and channel aging," *IEEE Trans. on Veh. Tech.*, 2017.
- [27] E. Björnson, M. Matthaiou, and M. Debbah, "Massive MIMO with non-ideal arbitrary arrays: Hardware scaling laws and circuit-aware design," *IEEE Trans. Wireless Commun.*, vol. 14, no. 8, pp. 4353–4368, Aug. 2015.
- [28] X. Zhang, M. Matthaiou, E. Björnson, M. Coldrey, and M. Debbah, "On the MIMO capacity with residual transceiver hardware impairments," in *Proc. IEEE Int. Conf. Commun.*. IEEE, 2014, pp. 5299–5305.
- [29] S. K. Sharma, A. Papazafeiropoulos, S. Chatzinotas, and T. Ratnarajah, "Impact of residual transceiver impairments on MMSE filtering performance of Rayleigh-product MIMO channels," in *IEEE Signal Processing Advances in Wireless Communications (SPAWC 2017)*, Japan, 2017.
- [30] E. Björnson, E. G. Larsson, and T. L. Marzetta, "Massive MIMO: Ten myths and one critical question," *IEEE Commun. Mag.*, vol. 54, no. 2, pp. 114–123, February 2016.
- [31] A. K. Papazafeiropoulos and T. Ratnarajah, "Deterministic equivalent performance analysis of time-varying massive MIMO systems," *IEEE Trans. on Wireless Commun.*, vol. 14, no. 10, pp. 5795–5809, Oct 2015.
- [32] C. Kong, C. Zhong, A. K. Papazafeiropoulos, M. Matthaiou, and Z. Zhang, "Effect of channel aging on the sum rate of uplink massive MIMO systems," in *IEEE Int. Symp. Information Theory (ISIT)*. IEEE, 2015, pp. 1222–1226.
- [33] A. Papazafeiropoulos, "Impact of user mobility on optimal linear receivers in cellular networks CSIT," in *Proc. IEEE Int. Conf. Commun.*, London, June 2015.
- [34] J. Hoydis, R. Couillet, and M. Debbah, "Asymptotic analysis of double-scattering channels," in *IEEE Conference Record of the Forty Fifth Asilomar Conference on Signals, Systems and Computers (ASILOMAR)*, 2011, pp. 1935–1939.
- [35] Z. Zheng, L. Wei, R. Speicher, R. R. Müller, J. Hämäläinen, and J. Corander, "Asymptotic analysis of Rayleigh product channels: A free probability approach," *IEEE Trans. on Inform. Theory*, vol. 63, no. 3, pp. 1731–1745, 2017.
- [36] M. Wu, D. Wuebben, A. Dekorsy, P. Baracca, V. Braun, and H. Halbauer, "Hardware impairments in millimeter wave communications using OFDM and SC-FDE," in *WSA 2016; 20th International ITG Workshop on Smart Antennas*, March 2016, pp. 1–8.
- [37] J. Chen and *et al.*, "Does LO noise floor limit performance in multi-Gigabit millimeter-wave communication?" *IEEE Microwave and Wireless Components Letters*, vol. PP, no. 99, pp. 1–3, 2017.
- [38] I. S. Gradshteyn and I. M. Ryzhik, "Table of integrals, series, and products," *Alan Jeffrey and Daniel Zwillinger (eds.)*, Seventh edition (Feb 2007), vol. 885, 2007.
- [39] A. Papazafeiropoulos, B. Clerckx, and T. Ratnarajah, "Rate-splitting to mitigate residual transceiver hardware impairments in massive MIMO systems," *IEEE Trans. on Veh. Tech.*, 2017.
- [40] M. Wenk, "MIMO-OFDM testbed: Challenges, implementations, and measurement results," Ph.D. dissertation, ETH ZURICH, 2010.
- [41] H. Holma and A. Toskala, *LTE for UMTS: Evolution to LTE-Advanced*, Wiley, Ed., 2011.
- [42] A. Lozano, A. M. Tulino, and S. Verdú, "High-SNR power offset in multiantenna communication," *IEEE Trans. Inform. Theory*, vol. 51, no. 12, pp. 4134–4151, 2005.
- [43] —, "Multiple-antenna capacity in the low-power regime," *IEEE Trans. Inform. Theory*, vol. 49, no. 10, pp. 2527–2544, 2003.
- [44] S. Verdú, "Spectral efficiency in the wideband regime," *IEEE T. Inform. Theory*, vol. 48, no. 6, pp. 1319–1343, 2002.
- [45] M. R. McKay, I. B. Collings, and A. M. Tulino, "Achievable sum-rate of MIMO MMSE receivers: A general analytic framework," *IEEE Trans. Inform. Theory*, vol. 56, no. 1, pp. 396–410, 2010.
- [46] S. Verdú, *Multuser detection*. Cambridge university press, 1998.
- [47] S. Chatzinotas and B. Ottersten, "Free probability based capacity calculation of multiantenna Gaussian fading channels with cochannel interference," *Physical Communication*, vol. 4, no. 3, pp. 206–217, 2011.
- [48] A. M. Tulino and S. Verdú, *Random matrix theory and wireless communications*. Now Publishers Inc., 2004, vol. 1, no. 1.
- [49] S. Jin, M. R. McKay, C. Zhong, and K. K. Wong, "Ergodic capacity analysis of amplify-and-forward MIMO dual-hop systems," *IEEE Trans. on Inform. Theory*, vol. 56, no. 5, pp. 2204–2224, 2010.
- [50] A. Prudnikov, Y. Brychkov, and O. Marichev, *Integrals and Series: More special functions*, ser. Integrals and Series. Gordon and Breach Science Publishers, 1990. [Online]. Available: <https://books.google.gr/books?id=OdS6QgAACAAJ>.
- [51] K. Petersen and M. Pedersen, "The matrix cookbook," *URL http://www2.imm.dtu.dk/pubdb/p.php*, vol. 3274, Nov. 2012.
- [52] H. Shin and M. Z. Win, "MIMO diversity in the presence of double scattering," *IEEE Trans. Inform. Theory*, vol. 54, no. 7, pp. 2976–2996, 2008.



Anastasios Papazafeiropoulos [S'06-M'10] is currently a Research Fellow in IDCOM at the University of Edinburgh, U.K. He obtained the B.Sc. in Physics and the M.Sc. in Electronics and Computers science both with distinction from the University of Patras, Greece in 2003 and 2005, respectively. He then received the Ph.D. degree from the same university in 2010. From November 2011 through December 2012 he was with the Institute for Digital Communications (IDCOM) at the University of Edinburgh, U.K. working as a postdoctoral Research

Fellow, while during 2012-2014 he was a Marie Curie Fellow at Imperial College London, U.K. Dr. Papazafeiropoulos has been involved in several EPSRC and EU FP7 HIATUS and HARP projects. His research interests span massive MIMO, 5G wireless networks, full-duplex radio, mmWave communications, random matrices theory, signal processing for wireless communications, hardware-constrained communications, and performance analysis of fading channels.



Shree Krishna Sharma (S'12-M'15) received the M.Sc. degree in information and communication engineering from the Institute of Engineering, Pulchowk, Nepal; the M.A. degree in economics from Tribhuvan University, Nepal; the M.Res. degree in computing science from Staffordshire University, Staffordshire, U.K.; and the Ph.D. degree in Wireless Communications from University of Luxembourg, Luxembourg in 2014. Dr. Sharma worked as a Research Associate at Interdisciplinary Centre for Security, Reliability and Trust (SnT), University of

Luxembourg for two years, where he was involved in EU FP7 CoRaSat project, EU H2020 SANSA, ESA project ASPIM, as well as Luxembourgish national projects Co2Sat, and SeMIGod. He is currently working as a Postdoctoral Fellow at Western University, Canada. His research interests include Internet of Things (IoT), cognitive wireless communications, Massive MIMO, Intelligent small cells, and 5G and beyond wireless systems.

In the past, Dr. Sharma was involved with Kathmandu University, Dhulikhel, Nepal, as a Teaching Assistant, and he also worked as a Part-Time Lecturer for eight engineering colleges in Nepal. He worked in Nepal Telecom for more than four years as a Telecom Engineer in the field of information technology and telecommunication. He is the author of more than 70 technical papers in refereed international journals, scientific books, and conferences. He received an Indian Embassy Scholarship for his B.E. study, an Erasmus Mundus Scholarship for his M. Res. study, and an AFR Ph.D. grant from the National Research Fund (FNR) of Luxembourg. He received Best Paper Award in CROWNCOM 2015 conference, and for his Ph.D. thesis, he received "FNR award for outstanding PhD Thesis 2015" from FNR, Luxembourg. He is a member of IEEE and has been serving as a reviewer for several international journals and conferences; and also as a TPC member for a number of international conferences including IEEE ICC, IEEE PIMRC, IEEE Globecom, IEEE ISWCS and CROWNCOM.



Tharmalingam Ratnarajah [A'96-M'05-SM'05] is currently with the Institute for Digital Communications, University of Edinburgh, Edinburgh, UK, as a Professor in Digital Communications and Signal Processing and the Head of Institute for Digital Communications. His research interests include signal processing and information theoretic aspects of 5G and beyond wireless networks, full-duplex radio, mmWave communications, random matrices theory, interference alignment, statistical and array signal processing and quantum information theory. He has

published over 300 publications in these areas and holds four U.S. patents. He was the coordinator of the FP7 projects ADEL (3.7M€) in the area of licensed shared access for 5G wireless networks and HARP (3.2M€) in the area of highly distributed MIMO and FP7 Future and Emerging Technologies projects HIATUS (2.7M€) in the area of interference alignment and CROWN (2.3M€) in the area of cognitive radio networks. Dr Ratnarajah is a Fellow of Higher Education Academy (FHEA), U.K..



Dr. Symeon Chatzinotas (S'06-M'09-SM'13) is currently the Deputy Head of the SIGCOM Research Group, Interdisciplinary Centre for Security, Reliability, and Trust, University of Luxembourg, Luxembourg. In the past, he has worked on numerous R&D projects for the Institute of Informatics Telecommunications, National Center for Scientific Research Demokritos, Institute of Telematics and Informatics, Center of Research and Technology Hellas, and Mobile Communications Research Group, Center of Communication Systems Research, University of

Surrey, Surrey, U.K. He has received the M.Eng. degree in telecommunications from Aristotle University of Thessaloniki, Thessaloniki, Greece, and the M.Sc. and Ph.D. degrees in electronic engineering from the University of Surrey, Surrey, U.K., in 2003, 2006, and 2009, respectively. Dr. Chatzinotas has more than 200 publications, 1600 citations and an H-Index of 22 according to Google Scholar. He is the co-recipient of the 2014 Distinguished Contributions to Satellite Communications Award, and Satellite and Space Communications Technical Committee, IEEE Communications Society, and CROWNCOM 2015 Best Paper Award. His research interests include multiuser information theory, co-operative/cognitive communications and wireless networks optimization.